# Negative-ion conversion of fluorine atoms in grazing scattering from a LiF(001) surface: A coupled cluster approach

A. G. Borisov, J. P. Gauyacq, and V. Sidis
*Laboratoire des Collisions Atomiques et Moléculaires,*
*Unité Mixte de Recherche CNRS-Université Paris-Sud (UMR8625), 91405 Orsay Cedex, France*

A. K. Kazansky
*Institute of Physics, St. Petersburg University, 198904 St. Petersburg, Russia*
(Received 28 June 2000; published 9 January 2001)

The $F^-$ ion formation from fluorine atoms in grazing scattering from a LiF(001) surface is studied. The coupled cluster treatment of the LiF target allows one to take into account the possible effect of the finite width of the valence band of the crystal on the negative-ion formation. The finite width of the valence band implies that the hole created in the crystal by electron transfer to the projectile can *a priori* migrate out of the charge transfer region thus promoting the negative-ion formation. We find that while *for the perfect crystal* the hole diffusion is rather fast, *in the case of a collision*, it is temporarily suppressed by the attractive Coulomb interaction between the hole and the negative ion in the final state of the charge transfer reaction. As a result, the charge transfer has a ''localized'' character and corresponds to binary-type electronic transitions between the projectile and the closest lattice sites along the trajectory.

DOI: 10.1103/PhysRevB.63.045407 PACS number(s): 79.20.Rf, 34.70.+e, 34.50.Dy

## I. INTRODUCTION

Recent experimental and theoretical studies on the interaction of charged and neutral projectiles with ionic crystal surfaces revealed the importance of the charge-transfer process between the projectile and the surface for various phenomena. The projectile-surface charge transfer not only determines the charge fractions in the scattered beams,[1–7] but it also serves as a precursor for electron emission,[8–11] population of surface excitons,[9,10] and sputtering of the target.[12–15] Moreover, the recent observation of discrete structures in the projectile energy-loss spectra have been explained as being due to successive electron capture-loss cycles.[9,10,16] (An extended review of the current status in the field can be found in Refs. 17 and 18.) It is thus important to understand the mechanisms underlying the electron capture and loss for the projectile moving in front of the surfaces of the ionic crystals.

Several possible mechanisms for the process of electron loss by the projectile have been proposed in the literature, taking into account the general suppression of the resonant electron loss by the broad band gap of the ionic crystal.[17,18] However, a comprehensive theoretical description free of adjustable parameters is still missing. The situation is quite different for electron capture from the valence band (VB) of ionic crystals where substantial progress in the description of the negative-ion formation[3,4,18–20] and neutralization of multiple- and singly-charged projectiles[14,15,20–22] has been achieved. In their present status, the theoretical models describing electron capture rely on specific properties of ionic crystals that we discuss in the example of the LiF crystal.

The LiF crystal is characterized by a flat and narrow (3.6 eV width) valence band separated from the conduction band by a broad band gap (14 eV). The LiF crystal has a negative electron affinity where 11.4–12 eV is enough to eject a VB electron into the vacuum while 14 eV is needed to excite the electron from the valence to the conduction band.[23–26] The negative (positive) charges are localized at the halogen (alkali) lattice sites. Owing to the localization of the VB electrons at the halogen sites, the process of electron capture by the projectile is usually described as being due to binary-type charge-transfer events between the projectile and the halogen sites of the crystal.[3,4,21,22] Furthermore, it is assumed that a hole created at a given halogen site by the removal of an electron will not be transferred to the other crystal sites on the time scale of the binary interaction. Therefore, the finite width of the VB is neglected. In recent work on the $H^+$ neutralization and $H^-$ formation in back scattering from the LiF(001) surface, another kind of charge-transfer interaction was considered by studying electron capture from electronic states delocalized in a small six atom cluster embedded in a point charge (PC) lattice.[20]

These different ''hole localization'' assumptions can be challenged if one considers the typical decay time of a hole created at a surface $F^-$ site as follows from the finite VB width (of the order of 50 a.u., see Sec. III A) and the typical travel time of a projectile over an $F^-$ site (of the order of 50 a.u. for a velocity of 0.1 a.u.). With this argument, one could say that the hole created at the anion surface site by electron transfer to the projectile would be able to move during the collision, thereby leading to noticeable perturbations of the binary-interaction picture. The effect of hole diffusion out of the charge-transfer region is to increase the negative-ion fraction in the scattered beam since it decreases the probability that the hole will be recaptured by the projectile. For very fast hole diffusion in the crystal (broad valence band), one should rather treat the charge transfer as the interaction between a state localized on the projectile and delocalized Bloch states of the crystal. For free-electron metals, this leads to the well-known exponential decay of the hole population on the projectile.[27]

It is the purpose of this paper to assess the validity of the

 

''localized hole'' approximation in the case of negative-ion formation in grazing scattering from a LiF(001) surface. As discussed in the conclusion, the results obtained here should be representative of any ionic crystal surface (alkali-halides, oxides). We have chosen the specific F/LiF(001) system for several reasons:

(i) Detailed experimental data are available on the $F^-$ ion fractions in grazing atom-surface scattering.[4,17]

(ii) A parameter-free study of the $F^-$ formation has been performed within the succession-of-binary-collisions model and ''localized hole'' approximation[19] that provides a basis for comparison.

(iii) Owing to the large electron affinity of fluorine (3.4 eV) and wide band gap of the LiF crystal, the electron loss from the $F^-$ ion is strongly suppressed at least at low-collision velocities. Therefore, the negative-ion fractions in the velocity region close to the negative-ion formation threshold ($v \sim 0.1$ a.u.) are mainly given by the electron-capture efficiency.

We use a time-dependent, coupled cluster approach based on a tight-binding description of the LiF target. The finite valence-band width, i.e., the hole diffusion in the crystal is explicitly included in the calculation.

The paper is organized as follows. In Sec. II, we describe the coupled cluster model with particular emphasis on the model for the energies of the different configurations. In Sec. III, the results and their discussion are presented, and, finally, Sec. IV is devoted to concluding remarks.

## II. THE COUPLED-CLUSTER MODEL

The coupled cluster approach, together with the tight-binding description of the target, has been intensively used at different levels of sophistication [from three-dimensional (3D) to linear chain model] to describe charge transfer in scattering or sputtering events.[28–32] In the present case, because of the closed-shell structure of the $F^-$ ion and of the localization of the VB electrons at the $F^-$ lattice sites of the LiF crystal, the problem of $F^-$ formation in grazing scattering from an LiF(001) surface can be cast in simple terms as a *hole transfer* from the fluorine projectile to the valence band of the LiF crystal. The problem is thus converted into a one-particle problem. To model the valence band of the LiF crystal, we consider the $Li^+$ ions as structureless positive point charges and we use a large cluster comprising $N = N_x N_y N_z$ halogen lattice sites. A schematic presentation of the model is given in Fig. 1. The size of the cluster is chosen large enough so that it does not influence the final $F^-$ fractions.

The tight-binding description of the charge-transfer problem between the projectile and the LiF cluster can be formulated in the diabatic basis of functions $\varphi_j$ corresponding to the hole location on the $p_X$, $p_Y$, or $p_Z$ orbitals of the projectile or of the crystal $F^-$ sites:

$$\varphi_j = \psi_{p_X}(\mathbf{R}_{j-1}), \quad j = 1,...,N+1,$$

$$\varphi_j = \psi_{p_Y}(\mathbf{R}_{j-N-2}), \quad j = N+2,...,2N+2,$$

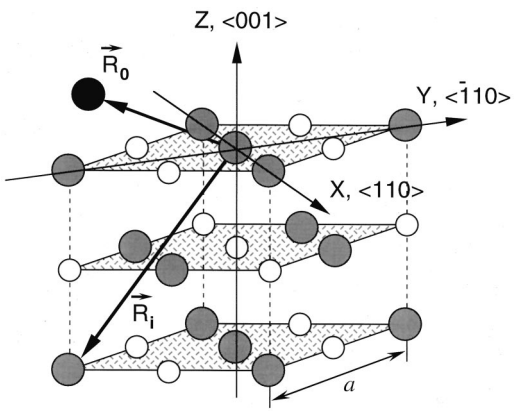


FIG. 1. Sketch of the considered system. The dark circles are used for the $F^-$ ions and the white circles are used for the $Li^+$ ions. The fluorine projectile is represented by the black circle. The upper shaded plane corresponds to the LiF(001) surface. The $\mathbf{R}_0$ vector gives the position of the projectile and the $\mathbf{R}_i$ vector gives the position of the $i$th $F^-$ lattice site. The *X*, *Y*, and *Z* axis coincide with crystallographic directions as indicated in the figure. $a = 7.59$ a.u. is the LiF lattice constant.

$$\varphi_j = \psi_{p_Z}(\mathbf{R}_{j-2N-3}), \quad j = 2N+3,...,3N+3, \tag{1}$$

where (see Fig. 1) $\mathbf{R}_0 = (X_0, Y_0, Z_0)$ is the position of the projectile and $\mathbf{R}_i$ $(i = 1,...,N)$ is the position of the $i$th halogen lattice site. Below we also use the notation $\mathbf{R}(j)$ $(j = 1,..,3N+3)$ where the relation between $\mathbf{R}(j)$ and $\mathbf{R}_i$ can be easily deduced from Eq. (1). $\psi_{p_X,p_Y,p_Z}(\mathbf{R})$ corresponds to the wave function of the fluorine atom located at $\mathbf{R}$ and bearing a hole in the $p_X$, $p_Y$, or $p_Z$ orbital, respectively. The initial states of the charge-transfer reaction (hole at the projectile) correspond to $\psi_{p_X,p_Y,p_Z}(\mathbf{R}_0)$, while the $\psi_{p_X,p_Y,p_Z}(\mathbf{R}_i)$ states $(i = 1,\ldots,N)$ correspond to the final state of the charge-transfer reaction with a hole located at a crystal site $\mathbf{R}_i$. The time-dependent wave function of the hole is given by

$$\Psi(t) = \sum_{j=1}^{3N+3} a_j(t)\varphi_j. \tag{2}$$

Substitution of Eq. (2) into the time-dependent Schrödinger equation leads to a system of coupled equations for the amplitudes $a_j(t)$:

$$i\frac{d}{dt}\mathbf{A}(\mathbf{t}) = \mathbf{H}(\mathbf{t})\mathbf{A}(\mathbf{t}), \tag{3}$$

where $\mathbf{A}(\mathbf{t})$ is the vector of coefficients $a_j$ and $\mathbf{H}(\mathbf{t})$ is the Hamiltonian matrix in the basis given by Eq. (1), its time dependence arises from the projectile motion. In deriving Eq. (3), we have assumed that the $\varphi_j$ basis is orthonormal. This limits the applicability of the present approach to not too small projectile surface separations where the time-dependent overlap between $\psi_{p_X,p_Y,p_Z}$ states centered at the projectile and at the lattice sites can be neglected.

Equations (1)–(3) form the basis of the coupled cluster approach. It consists of modeling the collisional system by a

finite cluster of anion sites of the LiF crystal and the projectile, and in evaluating the way a hole initially located on the projectile can jump on a surface site and further diffuse into the crystal. The various sites are coupled via (i) the projectile-anion sites charge-transfer interaction and (ii) the hopping integral between the crystal sites. We make the following assumptions concerning the structure of the Hamiltonian matrix:

(i) As shown in our previous study on $F^-$ formation in grazing scattering from the LiF(001) surface (succession of binary-collisions approach), the mixing of the projectile states by the field of the LiF crystal is small.[19] This is because of the total neutrality of the ionic crystal in the initial state so that the Coulomb potentials of the individual ions at the lattice sites are efficiently screened.[33] Therefore, we drop the corresponding terms in **H**.

(ii) Since the charge-transfer interaction between the projectile and the $i$th lattice site of the crystal decreases exponentially with the distance along the molecular axis: $R=|\mathbf{R}_0-\mathbf{R}_i|$,[19] we only include the couplings between the projectile and the lattice sites at the surface.

(iii) Only the hopping terms between nearest neighbors (eight at the surface and 12 in the bulk) are considered for the LiF crystal lattice sites. These hopping terms (coupled cluster) ensure the hole diffusion in the crystal.

### A. Energies of the states (diagonal elements)

In order to keep the discussion as simple as possible and concentrate on the basic physics underlying the relation between the hole diffusion and the charge-transfer process, we use here a simple (polarizable) point-charge (PC) model to determine the energies of the $\psi_{p_X,p_Y,p_Z}(\mathbf{R}_i)$ $(i=0,..,N)$ states. We adjust the parameters of our model in such a way that it reproduces the results of the self-consistent field Hartree-Fock-Roothaan (SCF) study performed in Ref. 19.

First, let us consider the terms corresponding to the hole located at the $p_X$, $p_Y$, or $p_Z$ orbital of the projectile in the initial state of the charge-transfer reaction: $E_j \equiv H_{jj}$ $(j=1, N+2,$ and $2N+3)$. The energy differences between these terms mainly arise from the interaction of the nonspherical charge density of the F-atom projectile with the field $j$ of the perfect LiF(001) crystal. Since $j$ quickly decreases with increasing projectile-surface distance $Z_0$, the corresponding energy differences are small[19] and will be neglected so that

$$E_j \equiv E_0(\mathbf{R}_0), \quad \text{where } j=1,\ N+2, \text{ and } 2N+3. \tag{4}$$

The $E_j \equiv H_{jj}$ $(j \neq 1, N+2,$ and $2N+3)$ energies correspond to the hole located at the $p_X$, $p_Y$, or $p_Z$ orbital of the F atom in the crystal in the final state of the charge-transfer reaction. Within the (polarizable) PC approximation one obtains:[18,19]

$$\Delta E_j \equiv E_j - E_0 = \Delta E_b + V^M + U_{\mathrm{LiF}}(\mathbf{R}_0) - \frac{1}{|\mathbf{R}_0-\mathbf{R}(j)|} + \Omega(\mathbf{R}_0,\mathbf{R}(j),j), \tag{5}$$

where $j \neq 1,\ N+2,\ 2N+3$. $\Delta E_b = A_{\mathrm{F/LiF}} - A_{\mathrm{F}}$ is the difference between the affinity of the F atom imbedded in the LiF crystal: $A_{\mathrm{F/LiF}}$ (the Madelung potential being subtracted) and the affinity of the free F-projectile: $A_{\mathrm{F}}=3.4$ eV. In the SCF study,[19] we obtained a small difference $\Delta E_b=-0.4$ eV, which basically reflects the fact that the $F^-$ ion structure is quite weakly perturbed when imbedded in the LiF lattice.[34]

$V^M$ stands for the Madelung potential created at the $F^-$ lattice site by the rest of the LiF crystal. The bulk value of the Madelung potential is 12.5 eV and it is reduced to 12.05 eV at the surface.

$U_{\mathrm{LiF}}(\mathbf{R}_0)$ is the interaction energy between the $F^-$ projectile and a perfect LiF(001) crystal. This exponentially decreases with increasing $Z_0$.[33]

The fourth term describes the attractive Coulomb interaction between the negatively charged projectile and the hole located at the $\mathbf{R}(j)$ lattice site.

$\Omega(\mathbf{R}_0,\mathbf{R}(j),j)$ represents the polarization interactions. It consists of ''atomic'' and ''collective'' parts. The ''atomic'' part takes into account the polarization of the $F^-$ ion projectile by the field of the hole located in the crystal (final state), as well as the polarization of the F atom located at a given lattice site by the field of the $F^-$ projectile (final state) and the polarization of the fluorine projectile by the field of the LiF crystal (initial state). These interactions are explicitly included in our treatment and serve to reproduce the SCF results for the energy differences. The polarizabilities $\alpha_{\mathrm{F}}=3.76a_0^3$, and $\alpha_{\mathrm{F}^-}=10.8a_0^3$ are taken from the literature.[35,36] The ''collective'' part corresponds to the response of the LiF crystal to the dipole field of the projectile and hole in the final state. The major consequences of the crystal response are the following:

(i) The attractive Coulomb interaction between the negative ion and the hole is screened.

(ii) The negatively charged projectile (final state of the charge-transfer reaction) interacts with its own image created by the polarization of the crystal.

For the projectile close to the $\mathbf{R}(j)$ surface site, i.e., for the range of distances where the charge transfer with this site is active, the negative charge merges with the hole as seen from the rest of the crystal. As explained in Refs. 15, 37, and 38, the effect of the crystal response vanishes for $\mathbf{R}(j)\rightarrow 0$. Therefore, we decided to neglect the ''collective'' part in $\Omega(\mathbf{R}_0,\mathbf{R}(j),j)$. The consequences of this approximation will be addressed in Sec. III.

The main contribution to $\Delta E_j$ comes from the attractive Coulomb interaction given by the fourth term in Eq. (5). This term leads to the energy level confluence between the initial and final states of the charge-transfer reaction reducing $\Delta E_j$ (see Fig. 2). This explains the low-velocity thresholds for the negative-ion formation in grazing scattering experiments despite the large asymptotic energy difference between the affinity level of the projectile and VB states.[3,19] There is one more important consequence of the long-ranged Coulomb term in the Eq. (5): the energy of the hole located at a given lattice site depends on the distance from the negatively charged projectile. This lifts the degeneracy of the $F^-$ sites of the crystal, introduces a local perturbation of the VB states, and as shown in Sec. III, this strongly reduces the effect of the hole diffusion on the negative-ion formation.

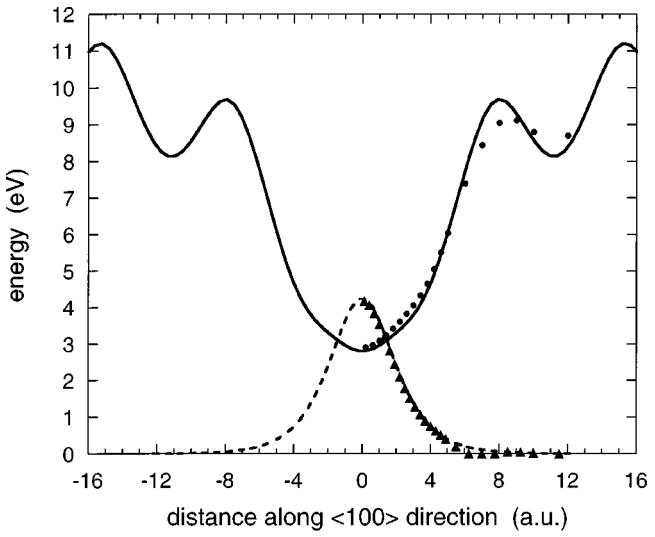


FIG. 2. The energy difference $\Delta E$ (solid line and circles) and hole transfer interaction $W_{\tilde{Z}\tilde{Z}}$ (dashed line and triangles) corresponding to the charge transfer between the projectile and a given $F^-$ site at the surface. The $F^-$ site is located at the coordinate origin (see Fig. 1). The data are presented as functions of the distance $d$ along the straight line trajectory in the $\langle 100\rangle$ direction: $\mathbf{R}_0=(X_0=d/\sqrt{2}, Y_0=d/\sqrt{2}, Z_0=3$ a.u.). Lines: model results given by Eqs. (7) and (11). Symbols: results of the SCF study of Ref. 19. For symmetry reasons we show the SCF data only for positive $d$.

### B. The charge-transfer interactions (nondiagonal elements)

First we discuss the charge-transfer interaction between the projectile and the halogen sites at the surface:

$$V_{nm}(\mathbf{R}_0,\mathbf{R}_i)=\langle \psi_{p_n}(\mathbf{R}_0)|H|\psi_{p_m}(\mathbf{R}_i)\rangle, \tag{6}$$

where $n, m=(X,Y,Z)$. The connection between $V_{nm}(\mathbf{R}_0,\mathbf{R}_i)$ and nondiagonal elements of the Hamiltonian $H_{kj}$ ($k$, $j=1,...,3N+3$) can be deduced from Eq. (1). We use earlier SCF results for the charge-transfer couplings.[19] For the range of the projectile-surface distances relevant for our study, these SCF data can be fitted with a simple analytical expression in the coordinate system with the $\tilde{Z}$ axis parallel to the molecular axis $\mathbf{R}_0-\mathbf{R}_i$ and the $\tilde{X}$ and $\tilde{Y}$ axis perpendicular to it (atomic units):

$$W_{\tilde{Z}\tilde{Z}}=-3.5\ \ \mathrm{e}^{-0.5R}/R^{1.47},$$

$$W_{\tilde{X}\tilde{X}}=V_{\tilde{Y}\tilde{Y}}=0.902\ \ \mathrm{e}^{-0.5R}/R^{1.01},$$

$$W_{kn}=0,\ \ k\neq n,\ \ k,n=(\tilde{X},\tilde{Y},\tilde{Z}), \tag{7}$$

where $R=|\mathbf{R}_0-\mathbf{R}_i|$ is the interatomic distance and the same notations as in Eq. (6) are used. The transformation from $W$ to $V$ is straightforward:

$$V_{nm}=\sum_{k=\tilde{X},\tilde{Y},\tilde{Z}}(\mathbf{e}_n\mathbf{e}_k)W_{kk}(\mathbf{e}_k\mathbf{e}_m), \tag{8}$$

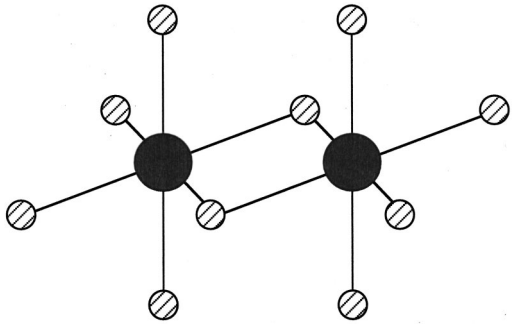

FIG. 3. The model $(Li_{10}F_2)^{8+}$ cluster used to calculate the hopping integrals between the $F^-$ sites of the crystal. Dark circles: $F^-$ ions; white circles: $Li^+$ ions.

where $\mathbf{e}_k$ is the unit length vector in $k$ direction and the quantities between the parenthesis are the scalar vector products. In deriving Eq. (8) we used the property of the $p$ orbitals: $\langle p_k|p_f\rangle=(\mathbf{e}_k,\mathbf{e}_f)$.

To obtain the hopping integrals between the nearest-neighbor $F^-$ lattice sites $\nu_{kj}\equiv\langle\varphi_k|H|\varphi_j\rangle$ we used a SCF method to calculate the electronic states of a $(Li_{10}F_2)^{8+}$ cluster embedded in the PC lattice (see Fig. 3). Then, as follows from the Koopman's theorem[39,40] the hopping integrals can be obtained from the energy differences of the corresponding orbitals.[19] We obtain the hopping integrals $\beta=-0.4494$ eV for the $p$ orbitals lying along the $\mathbf{R}(k)-\mathbf{R}(j)$ molecular axis. The hopping integrals for the orbitals lying in the plane perpendicular to the molecular axis are more than four times smaller and are neglected. The $\nu_{kj}$ hoppings can be obtained from

$$\nu_{kj}=(\mathbf{e}_k\mathbf{n})\beta(\mathbf{e}_j\mathbf{n}), \tag{9}$$

where $\mathbf{n}$ is the unit length vector along the line joining the two fluorine sites and $\mathbf{e}_k$ is the unit length vector along the $X$, $Y$, or $Z$ direction depending upon the $p$ orbital corresponding to the $\varphi_k$ basis state.

In Fig. 2 we present the energy differences $\Delta E_j$ and the couplings $W_{\tilde{Z}\tilde{Z}}$ for the projectile passing a given surface site at the fixed altitude $Z_0=3$ a.u.. The projectile moves above the $\cdots F^-Li^+F^-Li^+F^-\cdots$ row of ions in the $\langle 100\rangle$ direction. As one can see in the figure, model results obtained with Eqs. (5) and (7) reproduce the corresponding SCF data of the Ref. 19.

### C. The time propagation

With the definition of the energies and couplings given in Secs. II A and II B, the set of coupled equations (3) can be written in the form

$$i\frac{d}{dt}\mathbf{B}(t)=\tilde{\mathbf{H}}(t)\mathbf{B}(t), \tag{10}$$

where the components of the $\mathbf{B}$ vector are

$$b_j(t)=a_j(t)\exp\left[-i\int_0^t E_0(R_0(\tau))d\tau\right]. \tag{11}$$

The $\tilde{\mathbf{H}}$ matrix differs from the **H** matrix in Eq. (3) in that the diagonal elements are equal to $\Delta E_j = E_j - E_0(\mathbf{R}_0)$ instead of $E_j$.

For given initial conditions $\mathbf{B}_0 = \mathbf{B}(t=0)$, the time-dependent solution of the Eq. (10) can be obtained with Lanczos propagation technique.[41,42] Since the time propagation is done for a finite cluster size, care should be taken for possible artificial reflections from the cluster boundaries. Therefore, we have set the size of the cluster $N = N_X N_Y N_Z$ large enough so that the final $F^-$ fraction in the scattered beam does not depend on $N$.

## III. RESULTS AND DISCUSSION

### A. The valence-band structure of the model LiF cluster

First, we calculated the projected density of states (DOS) of the valence band for the surface and bulk $F^-$ sites in order to test the tight-binding description of the LiF crystal. The typical cluster size in these calculations is $61 \times 61 \times 61$ $F^-$ sites. The terms corresponding to the projectile are set to zero so that the Hamiltonian matrix $\tilde{\mathbf{H}}$ becomes independent of time, and only contains the hopping terms between nearest-neighbor sites as nondiagonal elements. The diagonal elements are degenerate and given by $(E_0 = 0)$: $\Delta E_j = E_j = V^M + A_{\mathrm{F/LiF}}$. This amounts to 15.5 eV for the halogen site in the bulk and 15.05 eV for the halogen site at the surface as follows from our SCF results. The initial wave function $\mathbf{B}_0(k)$ ($k = X$, $Y$, or $Z$) corresponds to the hole occupying the $p_X$, $p_Y$, or $p_Z$ orbital of the F atom at the center of the surface or in the middle of the cluster depending on whether we are interested in the projected DOS at the surface or in the bulk. First, the autocorrelation function $f_k(t)$ is obtained as a result of the time propagation:

$$f_k(t) = \mathbf{B}_0(k)^+ \mathbf{B}(t) = \mathbf{B}_0(k)^+ e^{-i\tilde{H}t} \mathbf{B}_0(k). \qquad (12)$$

Then the projected DOS $[N_k(\omega)]$ can be extracted as

$$N_k(\omega) = \frac{1}{\pi} \mathrm{Re}\left\{ \int_0^\infty f_k(t) e^{i(\omega + i\eta)t} dt \right\} \Bigg|_{\eta \to +0}. \qquad (13)$$

Because of the closed-shell structure of the $F^-$ orbitals forming the valence band of the LiF crystal, Koopman's theorem[39,40] can be used to relate the projected density of the hole states given by Eq. (13) and the projected density of electronic states $N_k^e(\omega)$: $N_k^e(\omega) = N_k(-\omega)$. In Fig. 4(a) we present the results for the projected DOS for the bulk and the surface: $N_X^e(\omega) + N_Y^e(\omega) + N_Z^e(\omega)$. In Fig. 4(b) we compare our results for the projected DOS in the bulk with experimental data.[24,25] A Gaussian broadening of the discrete states arising from the finite-cluster size was introduced. The broadening is 0.1 eV in Fig. 4(a). It is equal to 0.6 eV in Fig. 4(b) to take into account experimental broadening effects. We have verified that the results do not change when increasing each cluster dimension by a factor of 2.

As seen in the figures, the agreement between calculated and measured VB structures is good. The valence-band width, corresponding to the present tight-binding description

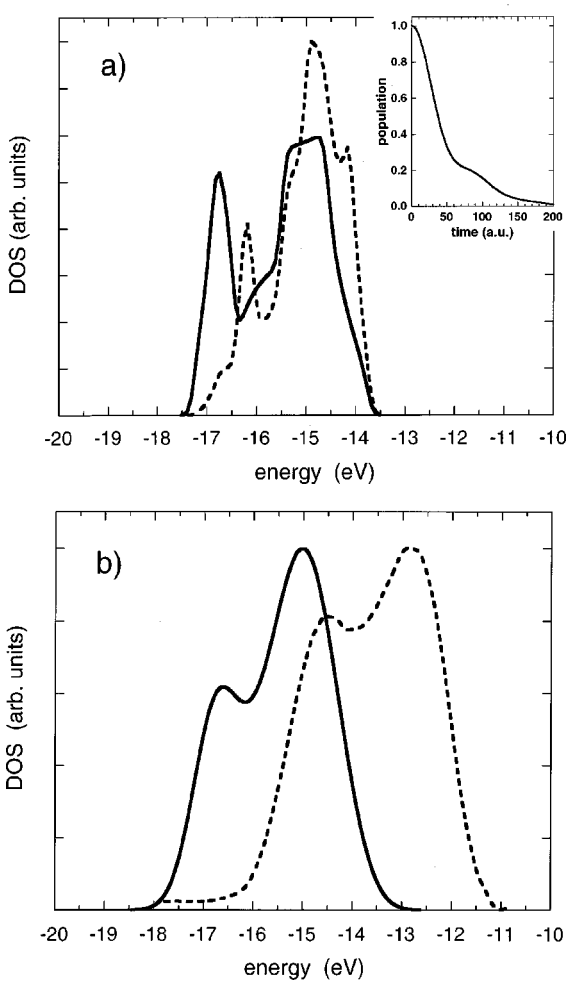


FIG. 4. (a) Projected DOS at the surface (dashed line) and in the bulk (solid line) obtained with the present tight-binding description of the LiF crystal. The inset shows the evolution of the hole population at the surface site as a function of time. Initially, the hole occupies the $p_Z$ orbital at this site. (b) The DOS in the valence band as measured in photoemission experiments (dashed line),[24,25] compared to the projected DOS in the bulk calculated from the present tight-binding model (solid line). The calculated DOS is broadened by 0.6 eV to account for experimental broadening.

is 3.8 eV that corresponds well to the available experimental[23–26] and theoretical[43–47] data. The top of the valence band is located at $-14$ eV with respect to the vacuum level. This is by $\sim 2$ eV larger than the experimentally measured ionization threshold. The difference primarily results from the neglect in the present model of the polarization interaction between the hole and the rest of the ionic crystal, the so-called Mott-Littleton energy.[48] Arguments for not including this term in the present study aiming to describe the negative-ion formation were given in the Sec. II A. In agreement with Ref. 47, we obtain that the peak structure at lower-binding energies is more pronounced for the surface-projected DOS. The shift between the surface and the bulk-projected DOS [Fig. 4(a)] reflects the 0.5 eV difference in the Madelung potentials at the surface and in the bulk.

In the inset of Fig. 4(a), we show the survival probability

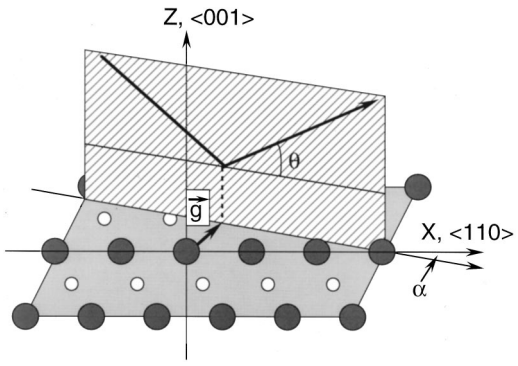


FIG. 5. Sketch of the grazing scattering of the fluorine projectile from the LiF(001) surface. The gray plane represents the LiF(001) surface with $F^-$ ions (black circles), and $Li^+$ ions (white circles). The hatched plane represents the scattering plane, the bold line indicating the projectile trajectory. $\theta$ is the incidence angle equal to the exit angle (we consider specular reflection) measured from the surface plane. $\alpha$ is the azimuthal angle with respect to the $\langle 110 \rangle$ direction. **g** is the impact parameter at the surface measured at the distance of closest approach.

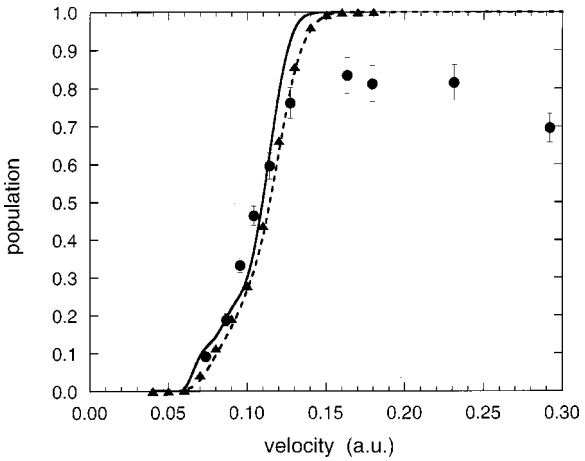


FIG. 6. Parallel velocity dependence of the negative ion formation probability in the outgoing beam for fluorine grazing scattering at LiF(001) surface. Dots with error bars represent experimental data of Ref. 4. Dashed line: results of the calculation based on the ''succession of binary collisions'' model with ''localized hole'' approximation.[19] Solid line: results of the full coupled cluster calculation. Triangles: results of the coupled cluster calculation where the hopping integrals between $F^-$ sites of the LiF crystal were set to zero.

of a hole initially occupying the $p_Z$ orbital at a surface $F^-$ site as a function of time. After 50 a.u. of time, the population at this surface site is reduced by more than a factor of 2 due to the hole transfer to the rest of the crystal. So, for the *unperturbed* LiF crystal, the hole diffusion is not slow compared to the characteristic time of the projectile passage over a given fluorine site (also of the order of 50 a.u.). Therefore the finite valence band width may have an effect on the charge transfer and cannot be neglected *a priori*. It is also worth noting that the population of a hole does not decay exponentially with time, thus forbidding the definition of a simple hole decay time.

### B. The negative-ion conversion of the neutral projectile

We have studied the $F^-$ formation from fluorine atoms for the grazing collision geometry presented in Fig. 5. The fluorine projectile is assumed to follow the $\mathbf{R}_0(t)=[X_{\rm ini}+v_\parallel t\cos\alpha,\ Y_{\rm ini}+v_\parallel t\sin\alpha, Z_0(t)]$ classical trajectory, where $\alpha$ is the angle of the trajectory with respect to the $\langle 110 \rangle$ direction at the surface, and $v_\parallel$ is the projectile velocity component parallel to the surface. The grazing angle of incidence $\theta=1.4°$ used in this study corresponds to the experimental conditions of Ref. 4. We have found that an angle $\alpha=4°$ well represents an experimental azimuthal random direction, in the sense that the final negative-ion fraction does not depend on $\alpha$ for $\alpha$ larger than 4°. The $Z_0(t)$ trajectory is obtained from the binary-interaction potentials between the projectile and the $Li^+$ and $F^-$ surface sites (for details see Ref. 19).

The time propagation of the wave function $\mathbf{B}(t)$ was performed with initial conditions corresponding to the hole located at the $p_X$ ($p_Y$ or $p_Z$) orbital of the projectile. The initial distance from the surface $Z_0(t=0)$ is chosen large enough so that the projectile and the surface sites are decoupled (typically $Z_0 \cong 10$ a.u.). As a result, we obtain the probability of $F^-$ formation in the outgoing trajectory path $P^-_{p_X,p_Y,p_Z}(\mathbf{g})$. Here, $p_X$, $p_Y$, or $p_Z$ corresponds to the initial condition, **g** is the impact parameter of the trajectory defined at the distance of closest approach (see Fig. 5). The final negative-ion fraction $P^-$ is obtained by averaging over all the initial conditions and impact parameters within the surface unit cell.

Final results for the $F^-$ formation in grazing scattering from the LiF(001) surface are presented in Fig. 6 together with experimental data of Refs. 4 and 17. The experimental negative-ion fractions close to the formation threshold are well reproduced by the present study. At large velocities, the theoretical results saturate at 100% while the measured negative ion fraction decreases as velocity increases. This shortcoming of the theory was already discussed in detail.[18] It is caused by the neglect of the electron loss by $F^-$ ion in the present calculations.

Now we turn to the discussion of the effect of the hole diffusion on the negative-ion formation. As the most important feature seen in Fig. 6, the coupled cluster results are very close to the results obtained within the ''succession of binary collisions'' model.[19] In this model, one sums the probabilities of electron capture by the projectile in individual binary collisions with $F^-$ lattice sites along the projectile path. These binary probabilities are obtained under the approximation that there is no hole diffusion in the crystal, i.e., the density of states in the valence band is approximated by the $\delta$ function. Therefore, it turns out that the hole diffusion has a very little effect on the negative-ion formation. It is then not surprising that convergence with the cluster size is reached with $N_X=351$, $N_Y=15$, $N_Z=2$ cluster. A large $N_X$ is necessary because of the long trajectory path of the projectile close to the surface, while $N_Z=2$ is certainly not enough to develop a valence-band structure of the crystal.

This feature of the ''hole localization'' during the charge transfer requires a more detailed discussion.

The question is then why are the coupled cluster results so close to those of the binary treatment neglecting the hole diffusion. In general, by introducing a coupled cluster, as done presently, several physical effects are included beyond the binary-type approximation: (i) The charge transfer can proceed simultaneously with several halogen sites at the surface. (ii) The hole diffusion may increase the negative-ion formation probability by removing a hole from the crystal sites coupled to the projectile so that it cannot be recaptured. In a certain sense, the latter effect amounts to confering a finite width to the states localized at the surface lattice sites: $E_j \rightarrow E_j - i\Gamma$.

We have checked the importance of (i) by performing a calculation with the hopping integrals between the crystal lattice sites set to zero, while the projectile states are still coupled to the states localized on the halogen surface sites. As one can see in Fig. 6, the results of this calculation are identical to the ones obtained with a binary treatment. Indeed, from the energy differences and couplings shown in Fig. 2, one can conclude that the charge transfer with a given lattice site is active in a rather small region around this site that barely overlaps with the charge-transfer region corresponding to the neighboring sites at the surface. As it follows from the comparison between the complete coupled cluster calculation and this model calculation, one can stress that introducing the finite valence-band width (hole diffusion) indeed increases the negative ion fraction, albeit this effect is very small.

Regarding (ii), the attractive Coulomb interaction between the negative ion and the hole in the final state of the charge-transfer reaction [see Eq. (5)] locally and temporarily perturbs the band structure and lifts the degeneracy between the crystal sites. Quantitative information can be obtained from the projected DOS shown in Fig. 7. It corresponds to the model situation when the projectile ($P$) is at a fixed distance from the surface $Z_0$ above a given ''active'' halogen site (HS). We present the sum of the DOS projected on the $\psi_{p_Z}(P)$ and on the $\psi_{p_Z}$(HS) states. Note that here we consider the DOS for the hole, in contrast to Fig. 4 where the electronic DOS has been plotted. Two calculations are performed. The adiabatic calculation is performed with the complete $\tilde{\mathbf{H}}$ matrix, while in the diabatic calculation, the coupling terms between the projectile and the surface sites were set to zero. As an energy reference we use the energy of the initial state, so that at infinite projectile surface separations, a projectile state is located at zero energy and the hole states of the VB are located at about $15 \pm 1.8$ eV. As soon as the projectile approaches the surface, the VB is perturbed and for decreasing projectile surface distance, discrete states split from the VB. In particular, one state that corresponds to the hole located at the HS is much lower in energy than the rest of the VB states. Close to the surface, the charge-transfer interaction between the $P$ and HS orbitals sets in and its effect is seen in the energy difference between the diabatic and adiabatic states, the latter repelling each other. Obviously, the hole transitions from the projectile or from the state associated with the HS to the other VB states are energetically unfavorable. Therefore, the charge transfer locally proceeds in a binary form involving only the projectile and the HS states. This information can be also inferred from the fact that a logarithmic scale for the projected DOS is needed to be able to observe the VB states at small projectile surface distances, which means that they are essentially decoupled from the projectile and from the ''active'' HS. Note that the situation could be different if one of the adiabatic states would enter the VB continuum. Then the hole loss from the adiabatic state to the VB would be possible via an adiabatic orbital promotion mechanism.[49–51] This is not the case in the present situation even for the projectile-surface distances $Z_0 = 2.8$ a.u. corresponding to the turning point of the trajectory in the considered velocity range. In fact, comparing diabatic and adiabatic projected DOS, one can see that when $Z_0$ decreases, the upper adiabatic state approaches the VB states and the relative weight of the latter in the DOS (correspondingly in the charge transfer) increases.

It is important to stress that our model, because of the neglect of the crystal polarization effects, *overestimates* the effect of the Coulomb potential of the projectile on the distant sites. This means that the VB *states* corresponding to lattice sites different from HS *are actually less perturbed* than it appears in Fig. 7. This brings them higher in energy (closer to the initial situation of large $Z_0$) and, correspondingly, this reinforces our conclusions on the suppression of the hole diffusion.

## IV. CONCLUSIONS

We have studied the $F^-$ formation in grazing scattering of fluorine atoms from an LiF(001) surface. The coupled cluster treatment of the projectile-surface charge-transfer problem allows us to take into account the finite valence-band width (hole mobility) of the target. The main purpose of this work is to elucidate the effect of hole diffusion in the LiF crystal on the negative-ion formation and to test the validity of previous treatments[3,4,19] based on the binary (projectile ''active site'' at the surface) collision model. For the *unperturbed* LiF crystal, the hole population left at the given anion surface site by electron transfer to the projectile decays on a 50 a.u. time scale. Since this time scale is comparable with the time of the projectile-surface site binary interaction, one could expect *a priori* that the hole migration out of the charge-transfer region would promote the negative ion formation.

The present model calculations are in good agreement with experimental data in the velocity range close to the negative-ion formation threshold. As a main result, we find that owing to the attractive Coulomb interaction between the hole in the crystal and the negative projectile in the final state of the charge-transfer reaction, the valence-band states are locally perturbed and the hole diffusion is temporarily inhibited during the collision. Basically, when the projectile is close to a given site at the surface (the ''active site''), the hole transfer proceeds between the projectile states and the ''active site'' states with very little hole delocalization in the

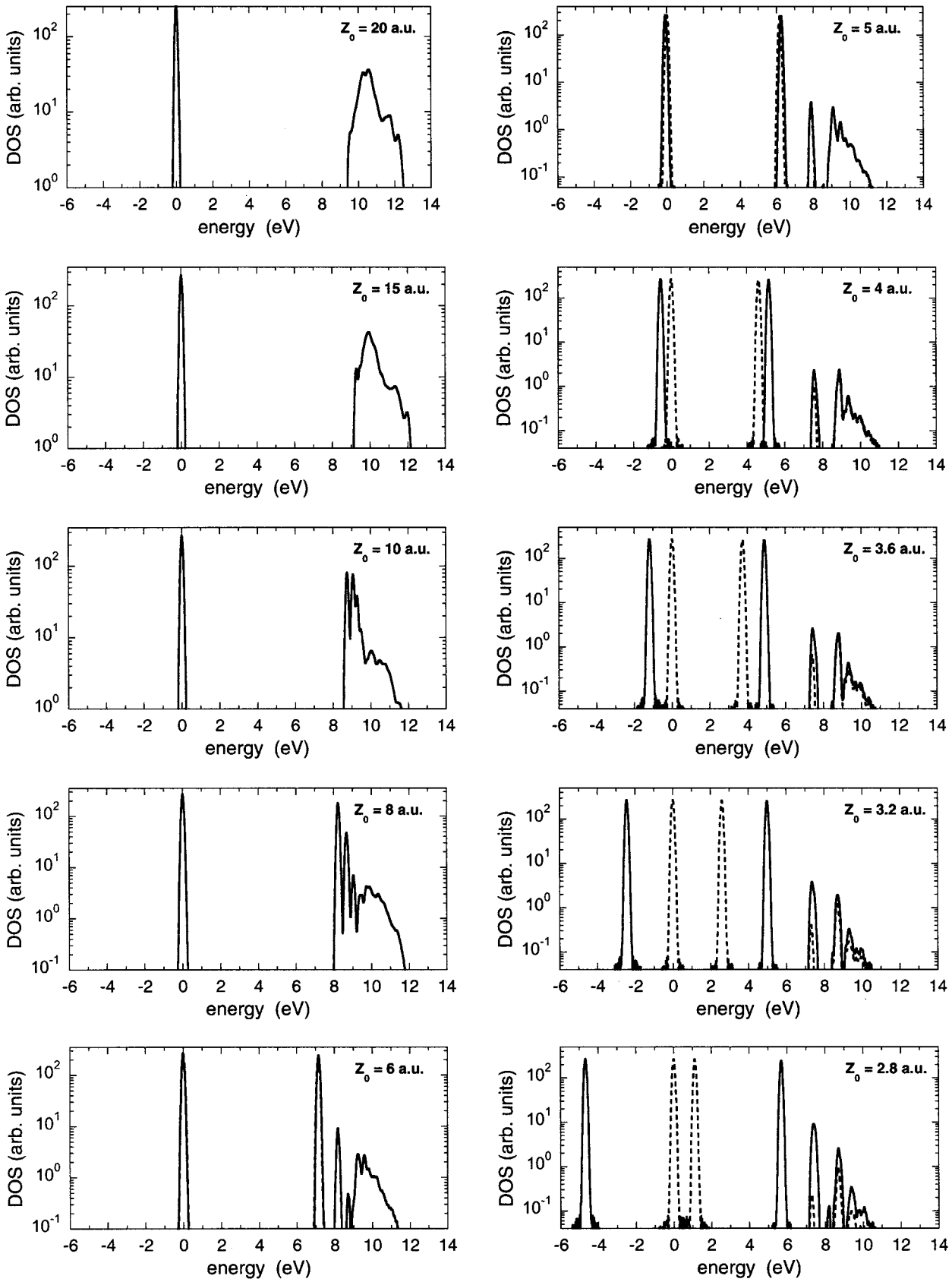


FIG. 7. Sum of the DOS projected on the $p_Z$ orbital of the projectile and $p_Z$ orbital of a given halogen site at the surface. The calculation is performed for the projectile fixed above this site at different altitudes $Z_0$. Solid and dashed lines correspond to the adiabatic and diabatic-type calculations, respectively. For further details see the text of the paper.

LiF crystal. Therefore, besides the slight increase of the negative-ion yield, the present results correspond well to the results of the earlier binary-collision treatments. We would like to emphasize that a local modification of the projectile and target states at the moment of the collision is often invoked to explain various phenomena in projectile-surface interactions.[20,49–51]

Although the absolute value of the effect of taking the hole diffusion into account might vary from one projectile/target combination to the other, the main conclusions obtained here should hold for the general case of the negative-ion formation at ionic crystal (alkali-halides, oxydes) surfaces. The mechanism of transient suppression of hole diffusion by the projectile field in the final state of the charge-transfer reaction is a robust consequence of the only partial screening of the time-dependent electric fields by the ionic crystal. Moreover, locally strong perturbation of the valence-band properties due to the Coulomb field of the projectile should play an important role in the case of multicharged ion projectiles. The situation should be quite different in the case of resonant neutralization of singly charged ions or Auger deexcitation of metastable species.[8,26] In this case, the final state of the projectile is neutral and thereby the valence-band structure is basically unperturbed and the hole diffusion out of the charge-transfer region is fast. Finally, the situation considered here is very different from the case of the projectile-metal surface interaction. For a metal target, the electron (hole) mobility is high and the long-range Coulomb fields are efficiently screened by the conduction electrons. The charge transfer is then nicely described as being due to the interaction with the continuum of the delocalized valence-band states (see e.g., Refs. 27, 52 and 53).


[1] R. Souda, K. Yamamoto, W. Hayami, B. Tilley, T. Aizawa, and Y. Ishizawa, Surf. Sci. **324**, L349 (1995).

[2] R. Souda, T. Suzuki, H. Kawanowa, and E. Asari, J. Chem. Phys. **110**, 2226 (1999).

[3] C. Auth, A. G. Borisov, and H. Winter, Phys. Rev. Lett. **75**, 2292 (1995).

[4] C. Auth, A. Mertens, H. Winter, A. G. Borisov, and V. Sidis, Phys. Rev. A **57**, 351 (1998).

[5] F. W. Meyer, Q. Yan, P. Zeijlmans van Emmichoven, I. G. Hughes, and G. Spierings, Nucl. Instrum. Methods Phys. Res. B **125**, 138 (1997).

[6] M. Maazouz, L. Guillemot, S. Lacombe, and V. A. Esaulov, Phys. Rev. Lett. **77**, 4265 (1996).

[7] S. Ustaze, R. Verucchi, L. Guillemot, and V. A. Esaulov, Phys. Rev. Lett. **79**, 3256 (1997).

[8] V. Kempter, Comments At. Mol. Phys. **34**, 11 (1998).

[9] P. Roncin, J. Villette, J. P. Atanas, and H. Khemliche, Phys. Rev. Lett. **83**, 864 (1999).

[10] H. Khemliche, J. Villette, P. Roncin, and M. Barat, Nucl. Instrum. Methods Phys. Res. B **164–165**, 608 (2000).

[11] P. Zeijlmans van Emmichoven, A. Niehaus, P. Stracke, F. Wiegershaus, S. Krischok, V. Kempter, A. Arnau, F. J. Garcia de Abajo, and M. Peñalba, Phys. Rev. B **59**, 10 950 (1999).

[12] N. Seifert, W. Husinsky, G. Betz, Q. Yan, and N. Tolk, Phys. Rev. B **51**, 12 202 (1995).

[13] P. Varga and V. Diebold, in *Low Energy Ion-Surface Interactions*, edited by J. W. Rabalais (Wiley, New York, 1994), p. 355.

[14] G. Hayderer, M. Schmid, P. Varga, H. P. Winter, F. Aumayr, L. Wirtz, C. Lemell, J. Burgdörfer, L. Hägg, and C. O. Reinhold, Phys. Rev. Lett. **83**, 3948 (1999).

[15] L. Wirtz, G. Hayderer, C. Lemell, J. Burgdörfer, L. Hägg, C. O. Reinholdt, P. Varga, H. P. Winter, and F. Aumayr, Surf. Sci. **451**, 197 (2000).

[16] C. Auth, A. Mertens, H. Winter, and A. G. Borisov, Phys. Rev. Lett. **81**, 4831 (1998).

[17] H. Winter, Prog. Surf. Sci. **63**, 177 (2000).

[18] A. G. Borisov and V. A. Esaulov, J. Phys.: Condens. Matter **12**, R177 (2000).

[19] A. G. Borisov and V. Sidis, Phys. Rev. B **56**, 10 628 (1997).

[20] E. A. García, P. G. Bolcatto, M. C. G. Passeggi, and E. C. Goldberg, Phys. Rev. B **59**, 13 370 (1999).

[21] L. Hägg, C. O. Reinhold, and J. Burgdörfer, Phys. Rev. A **55**, 2097 (1997).

[22] J. J. Ducrée, F. Casali, and U. Thumm, Phys. Rev. A **57**, 338 (1998).

[23] M. Piacentini and J. Anderegg, Solid State Commun. **38**, 191 (1981).

[24] F. J. Himpsel, L. J. Terminello, D. A. Lapiano-Smith, E. A. Eklund, and J. J. Barton, Phys. Rev. Lett. **68**, 3611 (1992).

[25] D. A. Lapiano-Smith, E. A. Eklund, and F. J. Himpsel, Appl. Phys. Lett. **59**, 2174 (1991).

[26] F. Wiegershaus, S. Krischok, D. Ochs, W. Maus-Friedrichs, and V. Kempter, Surf. Sci. **345**, 91 (1996).

[27] J. J. C. Geerlings and J. Los, Phys. Rep. **190**, 133 (1990).

[28] J. M. Feagin and K. H. Wanser, Phys. Rev. A **44**, 4228 (1991).

[29] K. L. Sebastian, Phys. Rev. B **31**, 6976 (1985).

[30] E. R. Gagliano, E. C. Goldberg, M. C. G. Passeggi, and J. Ferrón, Phys. Rev. B **31**, 6988 (1985).

[31] Y. Muda and D. M. Newns, Phys. Rev. B **37**, 7048 (1988).

[32] J. Merino, N. Lorente, M. Yu. Gusev, F. Flores, M. Maazouz, L. Guillemot, and V. A. Esaulov, Phys. Rev. B **57**, 1947 (1998).

[33] R. E. Watson, J. W. Davenport, M. L. Perlman, and T. K. Sham, Phys. Rev. B **24**, 1791 (1981).

[34] H. Tatewaki and E. Miyoshi, Surf. Sci. **327**, 129 (1995).

[35] S. H. Patil, Phys. Rev. A **46**, 3855 (1992).

[36] R. Medeiros, M. A. Castro, and O. A. V. Amaral, Phys. Rev. A **54**, 3661 (1996).

[37] W. B. Flower, Phys. Rev. **151**, 657 (1966).

[38] W. P. O'Brien, Jr. and J. P. Hernandez, Phys. Rev. B **9**, 3560 (1974).

[39] C. C. J. Roothaan, Rev. Mod. Phys. **23**, 69 (1951).

[40] T. Koopmans, Physica's Grav. **1**, 104 (1933).

[41] C. Leforestier, R. H. Bisseling, C. Cerjan, M. D. Feit, R. Friesner, A. Goldberg, A. Hammerich, G. Jolicard, W. Karrlein, H.-D. Meyer, N. Lipkin, O. Roncero, and R. Kosloff, J. Comput. Phys. **94**, 59 (1991).

[42] T. J. Park and J. C. Light, J. Chem. Phys. **85**, 5870 (1986).

[43] A. Zunger and A. J. Freeman, Phys. Rev. B **16**, 2901 (1977).

[44] A. B. Kunz, Phys. Rev. B **12**, 5890 (1975).
[45] E. L. Shirley, Phys. Rev. B **58**, 9579 (1998).
[46] E. L. Shirley, L. J. Terminello, J. E. Klepeis, and F. J. Himpsel, Phys. Rev. B **53**, 10 296 (1996).
[47] P. Wirz, J. Sarnthein, W. Husinsky, G. Betz, P. Nordlander, and Y. Wang, Phys. Rev. B **43**, 6729 (1991).
[48] G. D. Mahan, Phys. Rev. B **21**, 4791 (1980).
[49] L. Guillemot, S. Lacombe, V. A. Esaulov, E. Sanchez, N. Mandarino, V. N. Tuan, Yu. Bandourine, A. Daschenko, and V. Drobnich, Surf. Sci. **365**, 353 (1996).
[50] F. Xu, R. A. Baragiola, A. Bonanno, P. Zoccali, M. Camarca, and A. Oliva, Phys. Rev. Lett. **72**, 4041 (1994).
[51] K. Eder, D. Semrad, P. Bauer, R. Golser, P. Maier-Komor, F. Aumayr, M. Peñalba, A. Arnau, J. M. Ugalde, and P. M. Echenique, Phys. Rev. Lett. **79**, 4112 (1997).
[52] H. Shao, D. C. Langreth, and P. Nordlander, in *Low Energy Ion-Surface Interactions*, edited by J. W. Rabalais (Wiley, New York, 1994), p. 118.
[53] B. H. Cooper and E. R. Behringer, in *Low Energy Ion-Surface Interactions* (Ref. 52), p. 263.